Applied Physics Letters

Nitrogen-displacement-related electron traps in *n*-type GaN grown on a GaN freestanding substrate

Cite as: Appl. Phys. Lett. **118**, 012106 (2021); https://doi.org/10.1063/5.0035235
Submitted: 27 October 2020 • Accepted: 10 December 2020 • Published Online: 05 January 2021

Masahiro Horita, Tetsuo Narita, Tetsu Kachi, et al.

COLLECTIONS

EP This paper was selected as an Editor's Pick

ARTICLES YOU MAY BE INTERESTED IN

Progress on and challenges of p-type formation for GaN power devices
Journal of Applied Physics **128**, 090901 (2020); https://doi.org/10.1063/5.0022198

Study on shallow donor-type impurities of GaN epilayer regrown by epitaxial lateral overgrowth technique
Applied Physics Letters **118**, 012105 (2021); https://doi.org/10.1063/5.0033380

Vertical p-type GaN Schottky barrier diodes with nearly ideal thermionic emission characteristics
Applied Physics Letters **118**, 022102 (2021); https://doi.org/10.1063/5.0036093

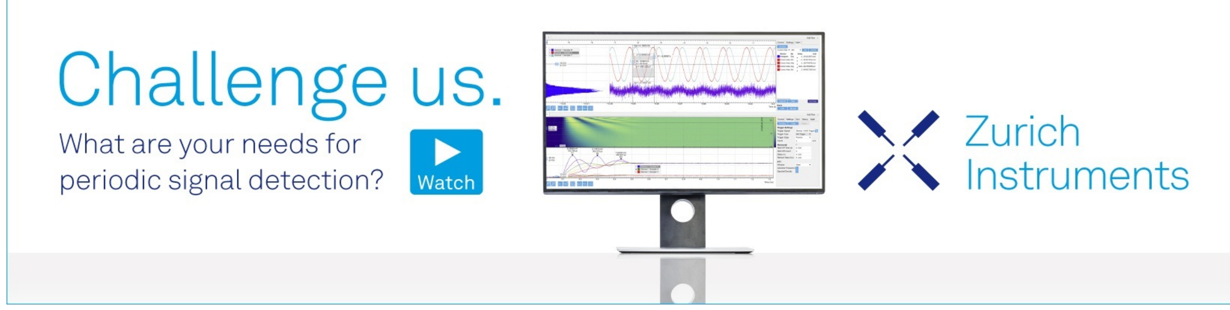

© 2021 Author(s).

Applied Physics Letters ARTICLE scitation.org/journal/apl

Nitrogen-displacement-related electron traps in *n*-type GaN grown on a GaN freestanding substrate

Cite as: Appl. Phys. Lett. **118**, 012106 (2021); doi: 10.1063/5.0035235
Submitted: 27 October 2020 · Accepted: 10 December 2020 ·
Published Online: 5 January 2021

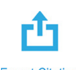

Masahiro Horita,[1,2,a)] Tetsuo Narita,[3] Tetsu Kachi,[2] and Jun Suda[1,2]

AFFILIATIONS

[1]Department of Electronics, Nagoya University, Furo-cho, Chikusa-ku, Nagoya, Aichi 464-8601, Japan
[2]Institute of Materials and Systems for Sustainability, Nagoya University, Furo-cho, Chikusa-ku, Nagoya, Aichi 464-8601, Japan
[3]Toyota Central R&D Labs., Inc., 41-1, Yokomichi, Nagakute, Aichi 480-1192, Japan

[a)]Author to whom correspondence should be addressed: horita@nagoya-u.jp

ABSTRACT

Energy levels due to intrinsic point defects are identified by deep-level transient spectroscopy (DLTS). Electron-beam (EB) irradiation created nitrogen vacancies (V_N) and nitrogen interstitials (N_I) in *n*-type GaN layers grown via metalorganic vapor phase epitaxy on freestanding GaN substrates, where the irradiation energies were selected to be within 100–401 keV to displace only nitrogen atoms in GaN. Two electron traps, EE1 (0.13 eV) and EE2 (0.98 eV), were observed in the DLTS spectra. The production rates of EE1 and EE2 were 0.093 and 0.109 cm^{-1} under 401 keV irradiation, which were nearly equal values. In the DLTS spectra recorded for EB-irradiated samples at the energy ranging from 100 to 401 keV, EE1 and EE2 were found to appear simultaneously at an irradiation energy of 137 keV and were observed at energies greater than 137 keV. On the basis of a comparison with the results of recent first-principles calculations, we attributed the EE1 and EE2 peaks to nitrogen vacancies V_N (+/0) and nitrogen interstitials N_I (0/−), respectively. Furthermore, annealing led to reductions of the densities of these traps at the same rate. The reduction of the densities of EE1 and EE2 can be explained by the migration of N_I and the subsequent recombination with V_N. The displacement energy of 21.8 eV for nitrogen in GaN was obtained from the irradiation-energy dependence of EE1.

Published under license by AIP Publishing. https://doi.org/10.1063/5.0035235

Gallium nitride (GaN) is one of the most promising materials for next-generation power devices because of its high breakdown electric field,[1] good mobility,[2,3] and high saturation velocity,[4] which have led to vertical GaN-based power field-effect transistors (FETs) with low energy consumption. Vertical power FETs such as heterojunction FETs and metal-oxide-semiconductor FETs have been reported by several groups.[5–9] Point defects in semiconductors strongly affect their material properties and, consequently, the device performance. In Si-based devices, the behavior of point defects has been extensively studied and the intentional introduction of defects has been used to enhance switching performance.[10,11] By contrast, the properties of point defects in GaN are not well understood. Various point defects are introduced during growth and device fabrication[12–14] and subsequently act as shallow levels (donors/acceptors), carrier traps, and/or recombination centers. If shallow levels or carrier traps are unintentionally introduced, the effective donor concentration varies. The doping level variation in the power device structure leads to degradation of the blocking voltage. Meanwhile, acceptor-like traps in *n*-type materials cause degradation of electron mobility because of an increase in ionized impurity scattering,[3] which results in an increase in the on-resistance. Understanding the relationship between point defects and energy states in the bandgap and controlling them are critical for the development of high-performance GaN power devices.

Electron-beam (EB) irradiation is an effective method for investigating intrinsic point defects. EB irradiation can introduce intrinsic point defects, i.e., vacancies and interstitials, intentionally without introducing impurity atoms, as demonstrated in other materials.[15–17] In the EB irradiation process, the concentration of point defects can be well controlled by the fluence and uniformly distributed in the depth direction because of the large penetration depth of the electron beam (~200 μm for 400 keV EB for GaN). Traps in EB-irradiated GaN have been studied by several groups by deep-level transient spectroscopy (DLTS).[18–25] In the early stage of these studies, several electron traps in the range of E_C − (0.06–0.20) eV, where E_C is the energy of the conductance-band minimum, were reported after 1–2.4 MeV EB irradiation of *n*-type GaN grown on sapphire substrates by metalorganic

vapor phase epitaxy (MOVPE), where some of the electron traps were severely overlapped.[18–23] A broad peak that consists of several deep electron traps in the range of $E_C - (0.7–1.2)$ eV has also been observed in n-type GaN grown by MOVPE on sapphire substrates.[21,23] One of the possibilities for multiple peaks is the overlap with the deep levels due to the threading dislocations originating from heteroepitaxy. In recent years, n-type GaN layers on freestanding GaN substrates with low threading dislocation densities have been used to investigate isolated point defects created via EB irradiation. Duc *et al.* reported three major electron traps with energy levels of $E_C - 0.15$ eV, $E_C - 0.8$ eV, and $E_C - 1.14$ eV in DLTS measurements of thick n-type GaN layers grown by hydride vapor phase epitaxy (HVPE) after 2 MeV EB irradiation.[25] In these previous studies, the authors suggested that a portion of the $E_C - (0.06–0.20)$ eV levels is related to nitrogen vacancies (V_N)[18,20,21,23,25] and that the $E_C - (0.7–1.2)$ eV levels are related to nitrogen interstitials (N_I)[21] or other intrinsic defects.[25] If V_N–N_I Frenkel pairs are produced by irradiation, the production rates of both peaks should be one-to-one. Even when homoepitaxial layers were used, however, the broad peaks exhibiting the multiple energy levels were observed, especially in the region $E_C - (0.7–1.2)$ eV, which makes discussing the production rates difficult. One possible cause of multiple peaks is that the EB irradiation displaced both Ga and N atoms, resulting in the formation of complexes.[19,20] Here, the EB irradiation energy strongly affects the introduced defect type. Look *et al.* reported that EB irradiation with an energy greater than 450 keV gives rise to the displacement of both Ga and N atoms.[26] The relationship between the threshold irradiation energy E_{th} for atom displacement and the displacement energy E_D is given by the following equation:[27]

$$E_D = \frac{2E_{th}(2mc^2 + E_{th})}{Mc^2}, \tag{1}$$

where M and m are the mass of the nucleus and electron, respectively, and c is the speed of light. As a result of theoretical calculations, E_D values of 22[28] and 17 eV[29] for Ga and 25[28] and 39 eV[29] for N were reported, which result in E_{th} values of 480 and 390 keV for Ga and 140 and 210 keV for N, respectively. These results suggest that low-energy EB irradiation between 100 and 400 keV can eliminate Ga displacement-related point defects and introduce only V_N–N_I Frenkel pairs. To simplify the system of intrinsic point defect production, detailed analysis of GaN with low-energy EB irradiation is essential. Fang *et al.* reported DLTS results for 400 keV EB-irradiated GaN; however, they used only one irradiation energy.[24]

In the present study, we performed EB irradiation with various energies less than 450 keV for n-type GaN grown on freestanding GaN substrates, which produces only N displacement. The production rates of irradiation-induced electron traps allow these traps to be assigned to V_N and N_I. Furthermore, thermal annealing demonstrates the reduction of these two traps at the same rate, which gives strong evidence that the electron traps originate from the Frenkel pairs. The displacement energy of N atoms was also obtained from the irradiation energy dependence of the V_N-related peak.

Si-doped n-type GaN layers were grown by MOVPE on HVPE-grown freestanding GaN substrates with a threading dislocation density of 3×10^6 cm^{-2}. Even if point defects are introduced along threading dislocations by EB irradiation, the trap density would be only 1.6×10^{14} cm^{-3} at most.[30] n-Type GaN with various Si concentrations was used, where the effective donor concentration ($N_{D,net}$), as evaluated by capacitance–voltage (C–V) measurements, was in the range of 2×10^{15} to 3×10^{16} cm^{-3} with a flat depth profile (see the supplementary material). The thickness of MOVPE-grown layers was 4 μm for the samples with $N_{D,net}$ less than 1×10^{16} cm^{-3} and 2 μm for the other samples. Secondary-ion mass spectrometry (SIMS) measurements indicated that the carbon impurity concentration was (2–3) $\times 10^{15}$ cm^{-3}. The oxygen impurity concentration was lower than the detection limit of the SIMS measurement (1×10^{16} cm^{-3}). EB irradiation was performed in the energy range of 100–401 keV and in the fluence range of (5.4–65) $\times 10^{15}$ cm^{-2} at room temperature, where samples were placed on a water-cooled metal plate. Ohmic contacts of Ti/Al with thicknesses of 20 nm/200 nm, respectively, were deposited onto the backside of the substrates by resistive heating evaporation and then sintered at 920 K for 5 min. This sintering was performed before the EB irradiation to avoid the migration and reaction of EB-induced point defects via annealing. Ni Schottky contacts with a thickness of 200 nm and a diameter of 1 mm were deposited by resistive heating evaporation after the EB irradiation. In the characterization by DLTS, first, temperature-scan DLTS and isothermal capacitance transient spectroscopy (ICTS) measurements were performed, where the maximum measurement temperature was limited to 370 K. This temperature limitation prevents the migration of EB-induced defects and enables the samples to be characterized in the irradiated state. The DLTS measurement with multicycle temperature scans was subsequently carried out with elevation of the maximum temperature. Because the sample was annealed at a temperature near the maximum temperature, the annealing behavior of traps can be evaluated by this method. DLTS measurements for electron traps were performed using a PhysTech HERA FT1234 instrument in conjunction with a Boonton 7200B capacitance meter. The reverse bias (V_R) was -5 V, and the filling plus voltage (V_P) of 0 V with a width t_p of 0.2 s was applied. The leakage current at V_R was less than 3 nA for all recorded Schottky barrier diodes in the temperature less than 370 K (see the supplementary material). The DLTS signals were obtained by deep-level transient Fourier spectroscopic analysis.[31] When the trap density was obtained from DLTS signals, we considered the so-called λ-effect. In addition, a GaN dielectric constant of $10.4\varepsilon_0$[32] and an electron density-of-states effective mass of $0.2m_0$[33] were employed, where ε_0 and m_0 are the permittivity of vacuum and the electron mass, respectively.

Figure 1 shows DLTS and ICTS spectra for as-grown and EB-irradiated GaN samples, where an EB irradiation energy (E_{irrad}) of 401 keV was used. In the spectra of the as-grown GaN samples, two electron traps, E1 and E3, located at $E_C - 0.24$ eV and $E_C - 0.56$ eV are observed, respectively; these traps have previously been observed in the spectra of MOVPE-grown GaN on freestanding GaN substrates.[34] After the EB irradiation, two trap levels, EE1 and EE2, were also observed, where EE1 was at the temperature of 123 K in the DLTS spectra and EE2 was at the time constant of 25 s in the ICTS spectra. These peaks appeared to be too broad to belong to a single discrete defect level; however, for the moment, we performed analyses for Arrhenius plots and trap densities using the peak top. Notably, the variation of the E3 peak intensities in Fig. 1 was not due to the EB irradiation but rather to the E3 variation in the as-grown samples because there are a certain degree of E3 trap density distributions in the samples of as-grown n-type GaN epilayers.[35] Figure 2 shows Arrhenius plots obtained from DLTS measurements in a wide temperature range. The activation energies were 0.13 and 0.98 eV, and the capture cross

Published under license by AIP Publishing

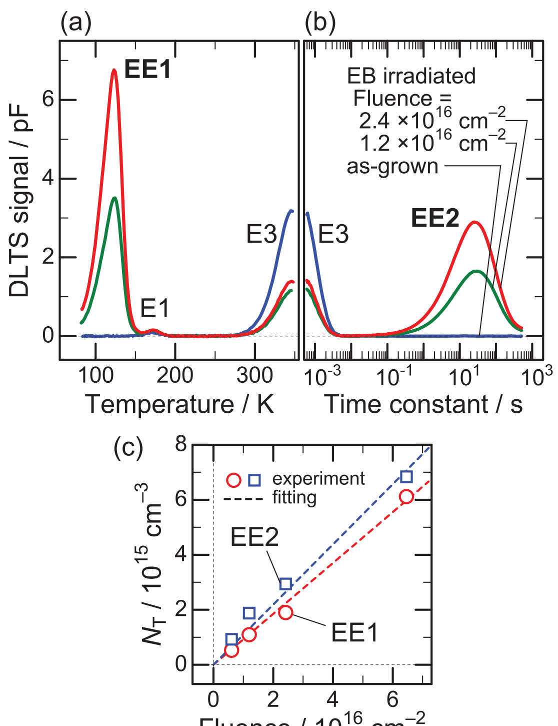

FIG. 1. (a) DLTS spectra for the time constant of $\tau = 1.63$ ms and (b) ICTS spectra for the temperature of $T = 370$ K; the as-grown *n*-type GaN sample ($N_{D,net} = 2 \times 10^{16}$ cm^{-3}) and samples after 401 keV EB irradiation at fluences of 1.2×10^{16} and 2.4×10^{16} cm^{-2} are shown. To avoid the migration of point defects, the measurement temperature was limited to 370 K, where a DLTS measurement was carried out for shallower trap levels and then an ICTS measurement was performed to detect deeper trap levels. (c) The densities (N_T) of EE1 and EE2 electron traps as a function of fluence for the EB-irradiated samples at the energy of 401 keV.

sections were 2×10^{-18} and 4×10^{-16} cm^2 for EE1 and EE2, respectively.

We now consider the trap density. The trap densities of both EE1 and EE2 linearly increased with increasing fluence of EB irradiation in the range of (5.4–65) $\times 10^{15}$ cm^{-3}, as shown in Fig. 1(c). The production rates, which are the ratio of the trap density to the fluence, for 401 keV EB irradiation were 0.093 and 0.109 cm^{-1} for EE1 and EE2, respectively. For each fluence sample, the densities of EE1 and EE2 were uniform in depth in the whole MOVPE-grown layer.

Here, we discuss the origin of the trap levels observed in the DLTS spectra. Recent first-principle calculations based on a hybrid functional, such as the calculations in studies on substitutional carbon on nitrogen sites, have accurately predicted carrier traps formed by point defects.[36–38] First-principles calculations based on the hybrid functional for vacancies and interstitials[39–43] are summarized in Table I. The energy levels of V_N and N_I were predicted to be E_C − (0.004–0.30) eV[39,41–43] and approximately E_C − 1 eV,[40,42] whereas those of V_{Ga} and Ga_I were E_C − (0.71–1.11) eV[42,43] and E_C − 0.94 eV,[42] respectively. The activation energies of EE1 and EE2 listed in Table II match the energy levels of V_N and N_I rather than those of V_{Ga} and Ga_I. Moreover, compared to the peaks at energies

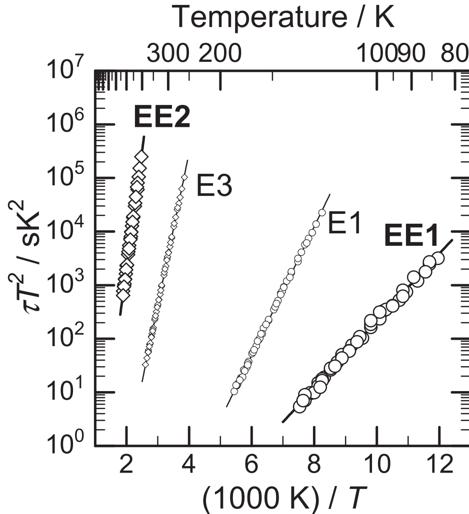

FIG. 2. Arrhenius plots of τT^2 for electron trap levels EE1 and EE2 observed in the *n*-type GaN sample ($N_{D,net} = 2 \times 10^{16}$ cm^{-3}) after EB irradiation (an E_{irrad} value of 401 keV and a fluence of 5.4×10^{15} cm^{-2}). The electron traps E3 and E1 are also shown for reference.

less than E_C − 0.7 eV reported in the previous studies, which are also listed in Table II, the EE2 peak had a narrow width and was not observed as apparent multiple peaks. Ga displacement was suppressed by the low-energy irradiation, as previously discussed, which resulted in peak narrowing. Therefore, the EE1 and EE2 peaks are most likely attributable to V_N (+/0) and N_I (0/−), respectively, which is supported by the observation that the production rates of EE1 and EE2 are approximately the same. Since the penetration depth of EB is much larger than the thickness of MOVPE-grown layers, V_N and N_I could be introduced uniformly in the whole MOVPE-grown layer, which results in the constant depth profiles of EE1 and EE2.

To determine the minimum irradiation energy for defect formation, we investigated the irradiation energy dependence. DLTS spectra of samples irradiated at various energies are presented in Fig. 3. The EE1 peak was not observed at 100 keV but appeared at 137 keV or higher EB energies. Because the threshold irradiation energy of N is lower than that of Ga, as previously discussed, this result supports the hypothesis that the origin of EE1 is V_N. By contrast, the EE2 peak appears to shift toward a longer time constant with decreasing E_{irrad}.

TABLE I. Calculated values (in eV) for the charge-transition level below the conduction-band minimum for intrinsic point defects in GaN, which are based on the hybrid functional. The highest levels of the charge transition for each point defect are shown.

	V_N (+/0)	N_I (0/−)	V_{Ga} (2−/3−)	Ga_I (2+/+)
Ref. 39	0.24	–	–	–
Ref. 40	–	1.01	–	–
Ref. 41	0.004	–	–	–
Ref. 42	0.30	0.99	0.71	0.94
Ref. 43	0.23	–	1.11	–

Published under license by AIP Publishing

TABLE II. Energy depth (in eV) of EB-induced electron traps below the conduction-band minimum obtained by DLTS measurements in this work and in previous studies by other groups.

	Irradiation energy	$E_C - (0.06–0.20\,\text{eV})$	$E_C - (0.7–1.2\,\text{eV})$
This work	137–401 keV	0.13 (EE1)	0.98 (EE2)
Ref. 23	0.25–2.5 MeV	0.20 (ER3)	0.72–1.02 (EEx1–4)
Ref. 24	0.4 MeV	0.18 (E)	0.9–1.0 (A_1), 1.2 (A_2)
Ref. 25	2 MeV	0.12 (D1)	0.89 (D5I), 1.14 (D6)

In addition, a small peak was observed at an E_{irrad} value of 100 keV. We speculated that the EE2 peak corresponds to at least two levels, where one is N_I and the other is a defect caused by low-energy EB irradiation. With increasing E_{irrad}, a trap level with a shorter time constant, which originates from N_I, becomes dominant. Although further investigation is needed to elucidate the details of EE2, we speculate that EE2 observed for the sample irradiated at 401 keV mainly arises from N_I.

Because the appearance of the EE1 peak is related to N displacement, the E_D value of N can be experimentally determined. From the E_{irrad} dependence of the EE1 production rates under the constant fluence shown in Fig. 3, E_{th} for N displacement was estimated to be 125 keV, which results in an E_D value of 21.8 eV for N according to Eq. (1).

Migration and annihilation of point defects through annealing at temperatures as high as 630 K were investigated by multicycle temperature scans in the DLTS measurements. Figure 4 shows DLTS spectra obtained by repeated measurements upon gradually raising the maximum temperature (T_{max}) for one Schottky barrier diode in an *n*-type GaN sample EB-irradiated at 401 keV. The EE1 and EE2 peaks were simultaneously decreased by annealing. In the relationship between the densities of EE1 and EE2 trap levels shown in the inset of Fig. 4, the density of EE2 was consistently higher than that of EE1. This trend may be due to the inclusion of defects other than N_I in the EE2 peak. Nevertheless, the reduction rate of EE2 was nearly equal to that of EE1, indicating annihilation of V_N and N_I in pairs, which supports the suggestion that the origins for EE1 and EE2 are V_N and N_I, respectively.

The migration barriers of V_N and N_I have been reported to be 4.0 and 1.6 eV, respectively, suggesting that N_I is mobile at temperatures near 473 K, whereas the migration barrier for V_N is too high for it to diffuse at similar temperatures.[44] These results suggest that the simultaneous reduction of EE1 and EE2 peaks was caused by the diffusion of N_I and the subsequent recombination with V_N. During the multiple temperature scans, the densities of E1 ($9.0 \times 10^{14}\,\text{cm}^{-3}$) and E3 ($8.2 \times 10^{15}\,\text{cm}^{-3}$) barely changed (the change was within 1%), whereas the concentrations of EE1 ($4.3 \times 10^{14}\,\text{cm}^{-3}$) and EE2 ($4.7 \times 10^{14}\,\text{cm}^{-3}$) were simultaneously reduced. Assuming that the migration length of N_I reaches several tens of nanometers during the DLTS measurements, this result means that N_I diffuses and recombines with V_N without any

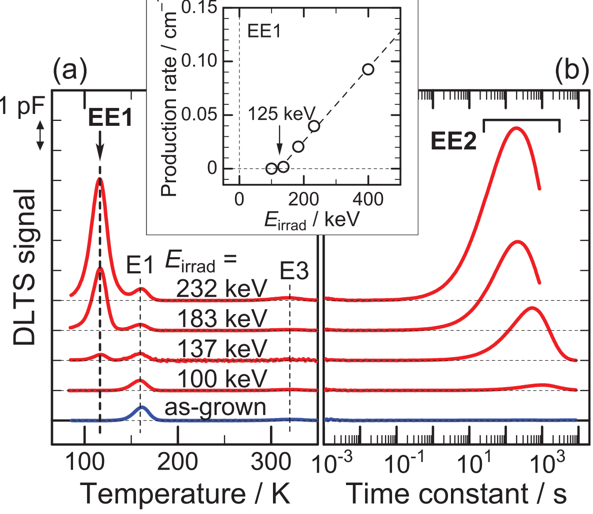

FIG. 3. Irradiation energy dependence of (a) DLTS ($\tau = 9.34$ ms) and (b) ICTS ($T = 360$ K) spectra for *n*-type GaN samples ($N_{D,net} = 2 \times 10^{15}\,\text{cm}^{-3}$). The fluence was fixed at $2 \times 10^{16}\,\text{cm}^{-2}$. The inset shows the E_{irrad} dependence of the production rates for EE1 under the constant fluence. The threshold of E_{irrad} for the appearance of EE1 was estimated by linear approximation.

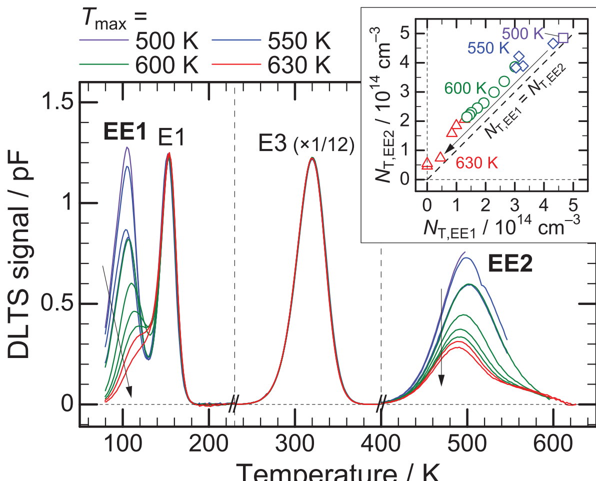

FIG. 4. Variation of the DLTS spectra resulting from multicycle temperature scans in the DLTS measurements for the *n*-type GaN sample ($N_{D,net} = 2 \times 10^{16}\,\text{cm}^{-3}$) after 401 keV EB-irradiation at a fluence of $5.4 \times 10^{15}\,\text{cm}^{-2}$. DLTS measurements with $\tau = 9.34$ ms were carried out 22 times in the range of 80 K to T_{max}, where T_{max} was gradually raised for each measurement. T_{max} was set to 500 K three times, 550 K five times, 600 K eight times, and then 630 K six times. As an approximation, the annealing time for temperatures greater than $T_{max} - 20$ K was 10 min. The inset shows the relationship between the trap densities of EE1 and EE2 for each measurement.

Published under license by AIP Publishing

reaction with the origin of E1 or E3, implying that the origin of E1 and E3 is not related to V_N. For E3 traps, this result is consistent with the reports that the E3 trap originates from Fe on a Ga site.[35,45]

In summary, EB irradiation with an energy less than 450 keV was performed for MOVPE-grown *n*-type GaN on freestanding GaN, where only N displacement occurred. Two electron trap levels, EE1 (0.13 eV) and EE2 (0.98 eV), were observed in DLTS spectra. The production rates of EE1 and EE2 were 0.093 and 0.109 cm^{-1} for 401 keV irradiation, which were almost the same values. From the irradiation energy dependence of the DLTS spectra, EE1 and the main component of EE2 appeared at the same energy of 137 keV. In addition, these peaks decreased in intensity at the same reduction rate during multicycle temperature scans in the DLTS measurements. These results indicate that the EE1 and EE2 peaks are mainly formed by V_N and N_I, respectively. Indeed, the EE1 and EE2 peaks include other low-intensity components that should be identified in future work. Nevertheless, it is notable that the origins of the main components of EE1 and EE2 have been clarified by experimental methods. The displacement energy of 21.8 eV for nitrogen in GaN obtained from the irradiation energy dependence is a critical value for simulations of defect formation in fabricated devices.

See the supplementary material for the current–voltage and *C*–*V* characteristics of Schottky barrier diodes for the as-grown and EB-irradiated GaN samples.

This work was supported by the Council for Science, Technology and Innovation (CSTI), Cross-ministerial Strategic Innovation Promotion Program (SIP), and "Next-generation power electronics—Research and Development of Fundamental Technologies for GaN Vertical Power Devices" (funding agency: NEDO).

DATA AVAILABILITY

The data that support the findings of this study are available from the corresponding author upon reasonable request.

REFERENCES

[1]T. Maeda, T. Narita, H. Ueda, M. Kanechika, T. Uesugi, T. Kachi, T. Kimoto, M. Horita, and J. Suda, in IEEE International Electron Devices Meeting (2018), Vol. 30.1.
[2]N. Sawada, T. Narita, M. Kanechika, T. Uesugi, T. Kachi, M. Horita, T. Kimoto, and J. Suda, Appl. Phys. Express **11**, 041001 (2018).
[3]H. Fujikura, T. Konno, T. Kimura, Y. Narita, and F. Horikiri, Appl. Phys. Lett. **117**, 012103 (2020).
[4]J. Liberis, M. Ramonas, O. Kiprijanovic, A. Matulionis, N. Goel, J. Simon, K. Wang, H. Xing, and D. Jena, Appl. Phys. Lett. **89**, 202117 (2006).
[5]M. Kanechika, M. Sugimoto, N. Soejima, H. Ueda, O. Ishiguro, M. Kodama, E. Hnyashi, K. Itoh, T. Uesugi, and T. Kachi, Jpn. J. Appl. Phys., Part 2 **46**, L503 (2007).
[6]H. Nie, Q. Diduck, B. Alvarez, A. P. Edwards, B. M. Kayes, M. Zhang, G. F. Ye, T. Prunty, D. Bour, and I. C. Kizilyalli, IEEE Electron Device Lett. **35**, 939 (2014).
[7]T. Oka, T. Ina, Y. Ueno, and J. Nishii, Appl. Phys. Express **8**, 054101 (2015).
[8]D. Shibata, R. Kajitani, M. Ogawa, K. Tanaka, S. Tamura, T. Hatsuda, M. Ishida, and T. Ueda, in IEEE International Electron Devices Meeting (2016), Vol. 10.1.
[9]Y. Zhang, M. Sun, D. Piedra, J. Hu, Z. Liu, Y. Lin, X. Gao, K. Shepard, and T. Palacios, in IEEE International Electron Devices Meeting (2017), Vol. 9.2.
[10]B. J. Baliga and E. Sun, IEEE Trans. Electron Devices **24**, 685 (1977).
[11]A. Mogrocampero, R. P. Love, M. F. Chang, and R. F. Dyer, IEEE Electron Device Lett. **6**, 224 (1985).
[12]F. D. Auret, S. A. Goodman, F. K. Koschnick, J. M. Spaeth, B. Beaumont, and P. Gibart, Appl. Phys. Lett. **74**, 2173 (1999).
[13]Z. Q. Fang, D. C. Look, X. L. Wang, J. Han, F. A. Khan, and I. Adesida, Appl. Phys. Lett. **82**, 1562 (2003).
[14]Y. Tokuda, in CS MANTECH Conference (2014), p. 19.
[15]J. Weber and M. Singh, Appl. Phys. Lett. **49**, 1617 (1986).
[16]D. Pons and J. C. Bourgoin, J. Phys. C **18**, 3839 (1985).
[17]C. Hemmingsson, N. T. Son, O. Kordina, J. P. Bergman, E. Janzen, J. L. Lindstrom, S. Savage, and N. Nordell, J. Appl. Phys. **81**, 6155 (1997).
[18]Z. Q. Fang, J. W. Hemsky, D. C. Look, and M. P. Mack, Appl. Phys. Lett. **72**, 448 (1998).
[19]S. A. Goodman, F. D. Auret, F. K. Koschnick, J. M. Spaeth, B. Beaumont, and P. Gibart, Mater. Sci. Eng., B **71**, 100 (2000).
[20]L. Polenta, Z. Q. Fang, and D. C. Look, Appl. Phys. Lett. **76**, 2086 (2000).
[21]Z. Q. Fang, L. Polenta, J. W. Hemsky, and D. C. Look, in 11th International Semiconducting and Insulating Materials Conference (2000), Vol. 35.
[22]S. A. Goodman, F. D. Auret, M. J. Legodi, B. Beaumont, and P. Gibart, Appl. Phys. Lett. **78**, 3815 (2001).
[23]S. A. Goodman, F. D. Auret, G. Myburg, M. J. Legodi, P. Gibart, and B. Beaumont, Mater. Sci. Eng., B **82**, 95 (2001).
[24]Z. Q. Fang, G. Farlow, B. Claflin, and D. Look, in 13th International Semiconducting and Insulating Materials Conference (2004), Vol. 29.
[25]T. T. Duc, G. Pozina, N. T. Son, E. Janzen, T. Ohshima, and C. Hemmingsson, Appl. Phys. Lett. **105**, 102103 (2014).
[26]D. C. Look, D. C. Reynolds, J. W. Hemsky, J. R. Sizelove, R. L. Jones, and R. J. Molnar, Phys. Rev. Lett. **79**, 2273 (1997).
[27]A. Ionascut-Nedelcescu, C. Carlone, A. Houdayer, H. J. von Bardeleben, J. L. Cantin, and S. Raymond, IEEE Trans. Nucl. Sci. **49**, 2733 (2002).
[28]J. Nord, K. Nordlund, J. Keinonen, and K. Albe, Nucl. Instrum. Methods Phys. Res., Sect. B **202**, 93 (2003).
[29]H. Y. Xiao, F. Gao, X. T. Zu, and W. J. Weber, J. Appl. Phys. **105**, 123527 (2009).
[30]T. Narita, K. Tomita, K. Kataoka, Y. Tokuda, T. Kogiso, H. Yoshida, N. Ikarashi, K. Iwata, M. Nagao, N. Sawada, M. Horita, J. Suda, and T. Kachi, Jpn. J. Appl. Phys., Part 1 **59**, SA0804 (2020).
[31]S. Weiss and R. Kassing, Solid-State Electron. **31**, 1733 (1988).
[32]A. S. Barker and M. Ilegems, Phys. Rev. B **7**, 743 (1973).
[33]I. Vurgaftman, J. R. Meyer, and L. R. Ram-Mohan, J. Appl. Phys. **89**, 5815 (2001).
[34]Y. Tokuda, ECS Trans. **75**, 39 (2016).
[35]M. Horita, T. Narita, T. Kachi, and J. Suda, Appl. Phys. Express **13**, 071007 (2020).
[36]J. L. Lyons, A. Janotti, and C. G. Van de Walle, Phys. Rev. B **89**, 035204 (2014).
[37]M. A. Reshchikov, M. Vorobiov, D. O. Demchenko, U. Ozgur, H. Morkoc, A. Lesnik, M. P. Hoffmann, F. Horich, A. Dadgar, and A. Strittmatter, Phys. Rev. B **98**, 125207 (2018).
[38]T. Narita, K. Tomita, Y. Tokuda, T. Kogiso, M. Horita, and T. Kachi, J. Appl. Phys. **124**, 215701 (2018).
[39]Q. M. Yan, A. Janotti, M. Scheffler, and C. G. Van de Walle, Appl. Phys. Lett. **100**, 142110 (2012).
[40]H. J. von Bardeleben, J. L. Cantin, U. Gerstmann, A. Scholle, S. Greulich-Weber, E. Rauls, M. Landmann, W. G. Schmidt, A. Gentils, J. Botsoa, and M. F. Barthe, Phys. Rev. Lett. **109**, 206402 (2012).
[41]M. A. Reshchikov, D. O. Demchenko, J. D. McNamara, S. Fernandez-Garrido, and R. Calarco, Phys. Rev. B **90**, 035207 (2014).
[42]J. L. Lyons and C. G. Van de Walle, npj Comput. Mater. **3**, 12 (2017).
[43]M. Matsubara and E. Bellotti, J. Appl. Phys. **121**, 195701 (2017).
[44]S. Limpijumnong and C. G. Van de Walle, Phys. Rev. B **69**, 035207 (2004).
[45]Y. Zhang, Z. Chen, W. Li, H. Lee, M. R. Karim, A. R. Arehart, S. A. Ringel, S. Rajan, and H. Zhao, J. Appl. Phys. **127**, 215707 (2020).

Published under license by AIP Publishing